Epidote U-Pb ages vs. fluid-mineral interaction

Peverelli V.[1], Berger A.[1], Lanari P.[1], Wille M.[1], Villa I.M.[1,2], Rubatto D.[1,3], Pettke T.[1] & Herwegh M.[1]

[1]University of Bern
[2]University of Milano-Bicocca
[3]University of Lausanne

Corresponding author: veronica.peverelli@geo.unibe.ch

EGU General Assembly #vEGU21 19-30 April 2021

1 Introduction

The application of U-Pb geochronology by LA-ICP-MS to minerals of the epidote-clinozoisite solid solution [1] allows to determine the timeframe of low-T deformation. Although the closure temperature of epidote is ca. 685-750 °C [2], resetting of the U-Pb isotopic system can occur via fluid-mineral interaction even at lower temperatures.

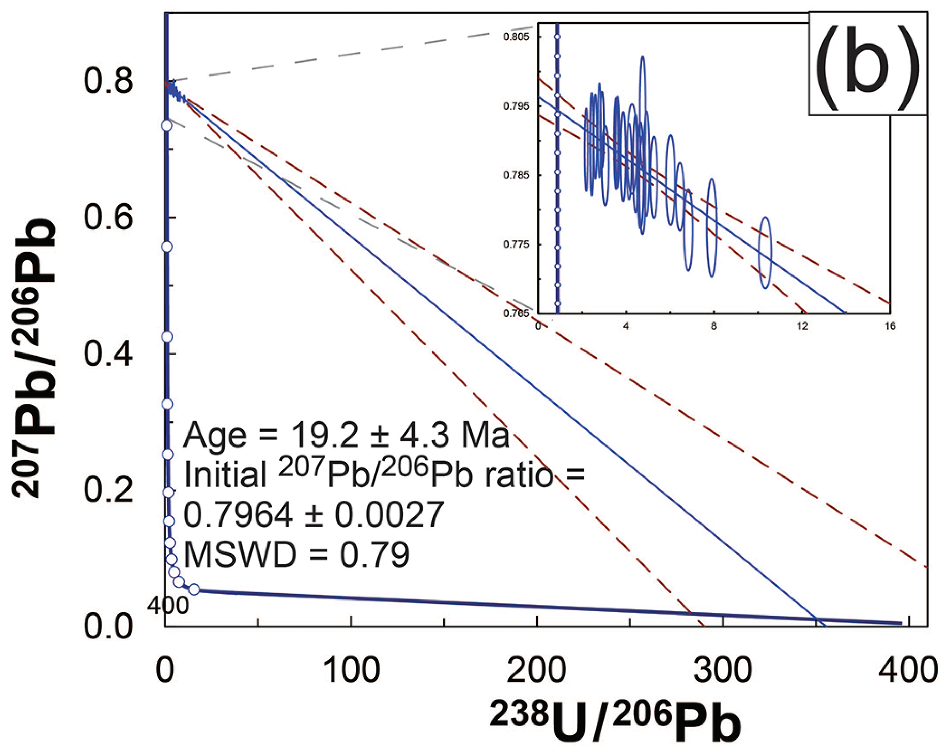

Fig. 1- Tera-Wasserburg plot of the studied sample; modified from [1].

LA-ICP-MS (i.e. in-situ) U-Pb isotopic data of Epidote-A (Figs. 2-3) yield a Miocene age and indicate only one epidote generation (Fig. 1): dating the crystallization of Epidote-A or subsequent fluid-mineral interaction?

Assessment of U-Pb isotopic data vs. microstructures, and additional geochemical and isotopic data is key to ascertain whether the calculated U-Pb ages date the crystallization of epidote or its subsequent interaction with a fluid during deformation.

2 Studied sample

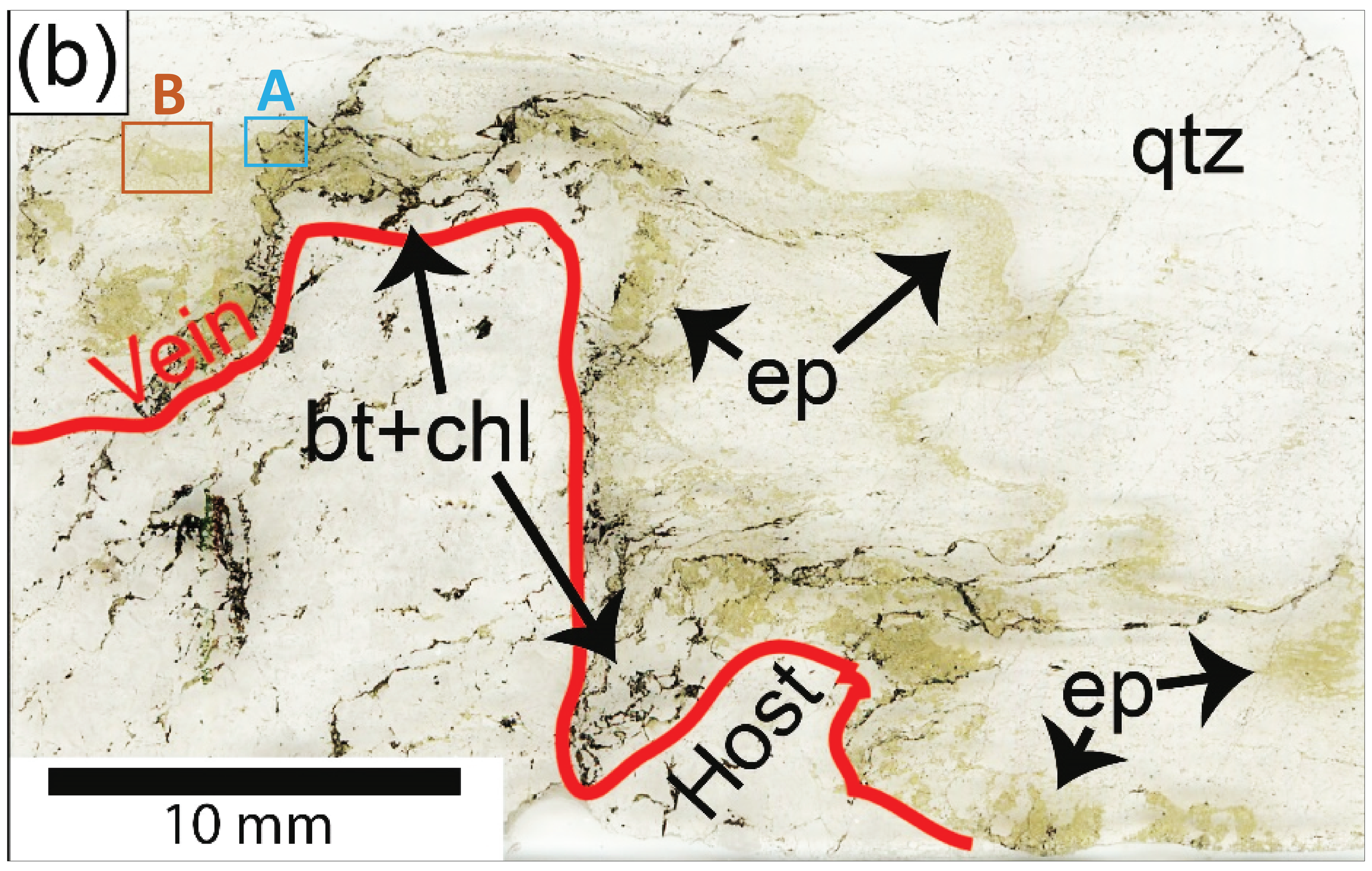

Fig. 2- Plane-light scan of the studied thin section; modified from [1].

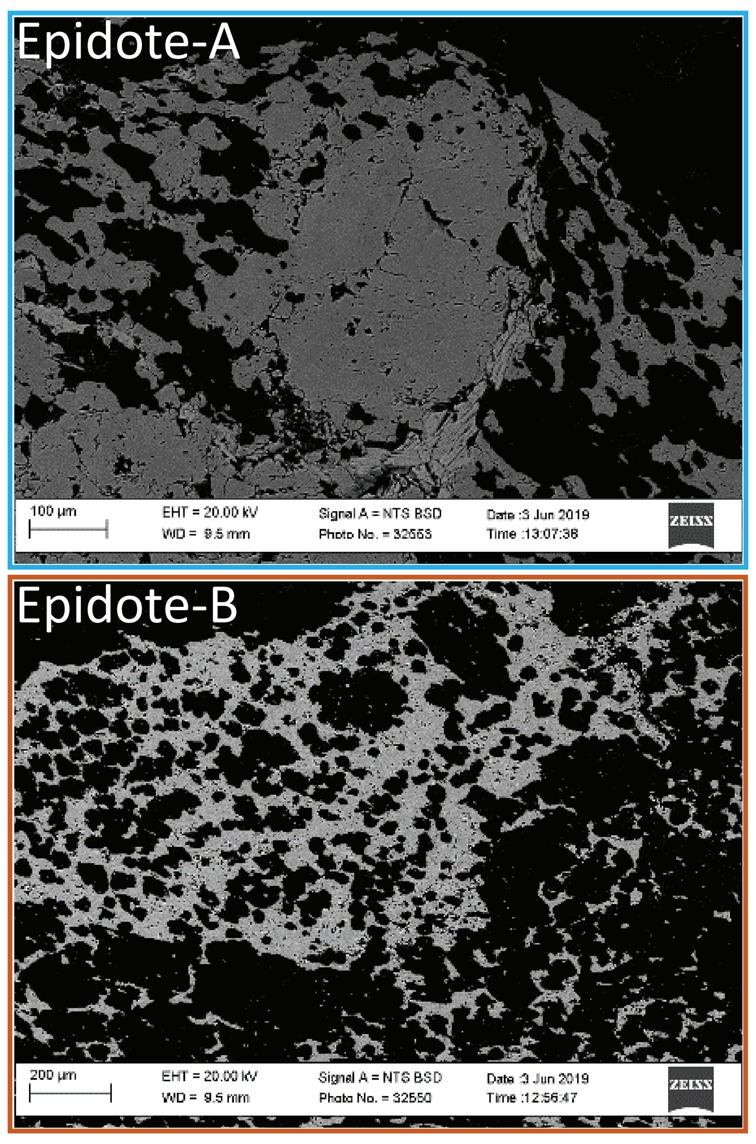

Fig. 3- BSE images of Epidote-A (above) and -B (below).

Folded epidote +qtz+bi±chl vein (Fig. 2) sampled at Grimsel Pass (Central Swiss Alps) hosted by the Central Aar Granite [1].

Petrography:
1) Epidote-A (Fig. 3, above): an-/subehdral porous grains of 0.1-1 mm in size; porous and associated with green biotite and rare chlorite, whose formation is consistent with the Handegg phase (22-17 Ma) of Alpine history [3].
2) Epidote-B (Fig. 3, below): anhedral grains sized < 0.1 mm; in "spongy" domains with dynamically recrystallized (SGR) quartz or mantling (i.e. younger than) Epidote-A.

3 Evidence for secondary fluid

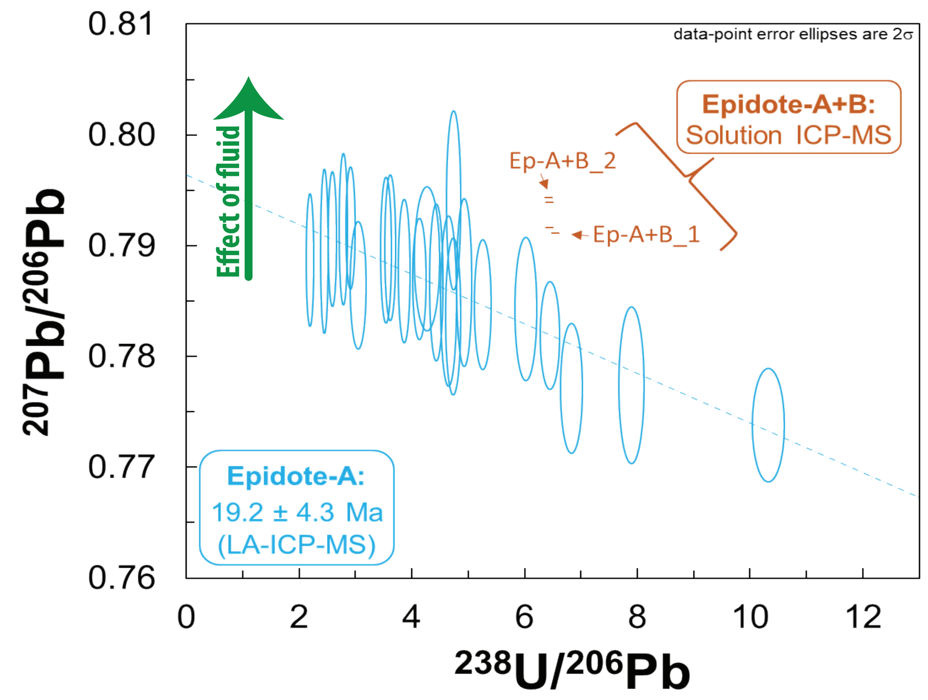

Fig. 4- Tera-Wasserburg diagram of Epidote-A LA-ICP-MS U-Pb data and solution ICP-MS U-Pb data of Ep-A+B microseparates.

Ep-A+B_1 and Ep-A+B_2 = epidote microseparates obtained by crushing vein material; representing mixtures of Epidote-A and -B in varying proportions, as no physical separation of pure Epidote-B is possible. $^{238}U/^{206}Pb$ and $^{207}Pb/^{206}Pb$ ratios of epidote in the microseparates are measured by solution ICP-MS, and then plotted in a Tera-Wasserburg diagram with the LA-ICP-MS analyses of Epidote-A. U-Pb data show differences between Epidote-A and -B, hinting at the addition of external Pb via a secondary fluid.

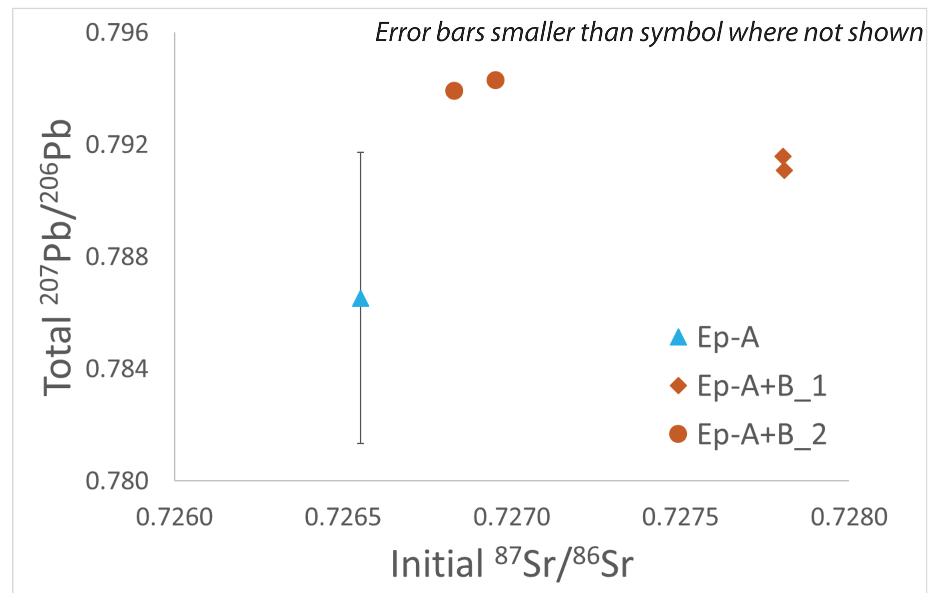

Fig. 5- Pb and Sr isotopic data of Epidote-A and Ep-A+B microseparates.

Variability in Sr isotopic data (Fig. 5) might be due to biotite contamination, yet to be ascertained.

4 Significance of U-Pb age of Epidote-A

- U-Pb age of 19.2 ± 4.3 Ma [1], consistent with the Handegg phase (22-17 Ma) of Alpine deformation [3].
- Associated with green biotite = stable phyllosilicate during the Handegg phase [3].
- Only rare chlorite = stable phyllosilicate during the Oberaar phase (14-3.5 Ma) of Alpine deformation [3].
- Low MSWD of the Tera-Wasserburg regression (Fig. 1) indicates only one epidote generation in Epidote-A.

U-Pb age of Epidote-A dates crystallization during the Handegg phase. No evidence for isotopic resetting of the U-Pb system is observed, despite the subsequent ingression of a secondary fluid.

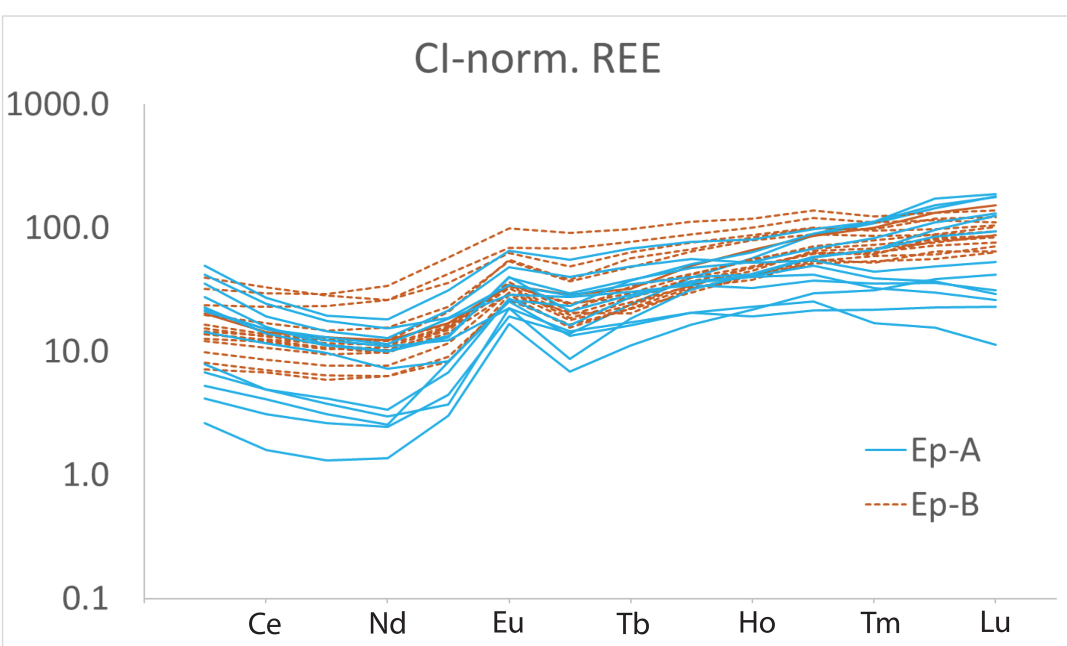

Fig. 6- CI chondrite-normalized REE patterns of the analyzed epidote vein.

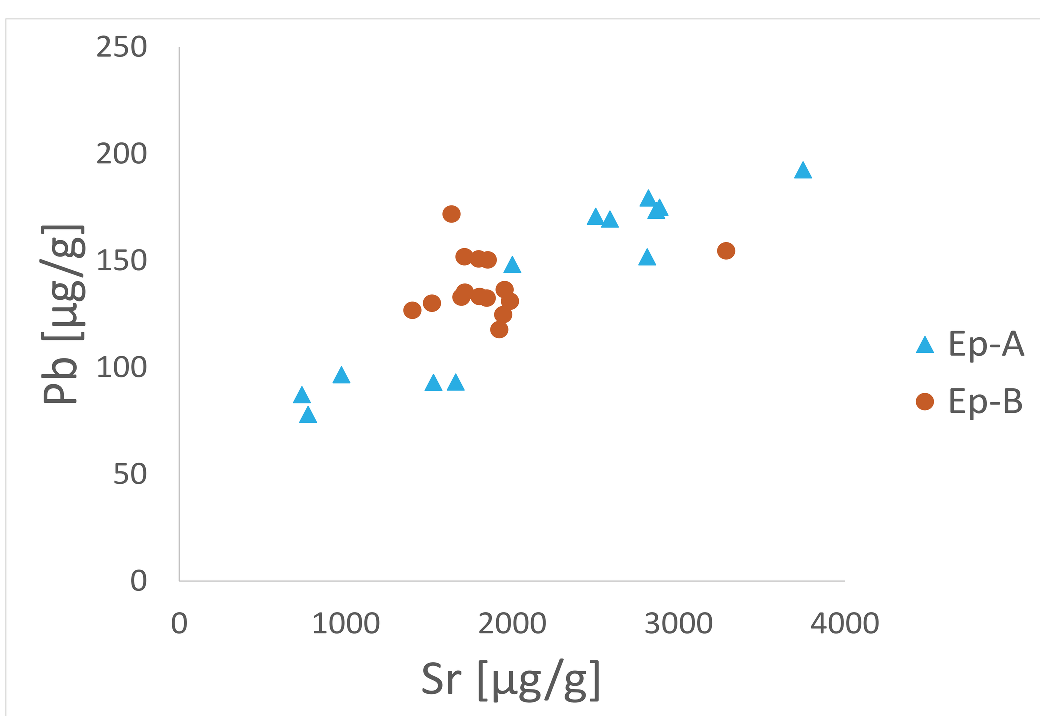

Fig. 7- Pb and Sr contents of the analyzed epidote vein.

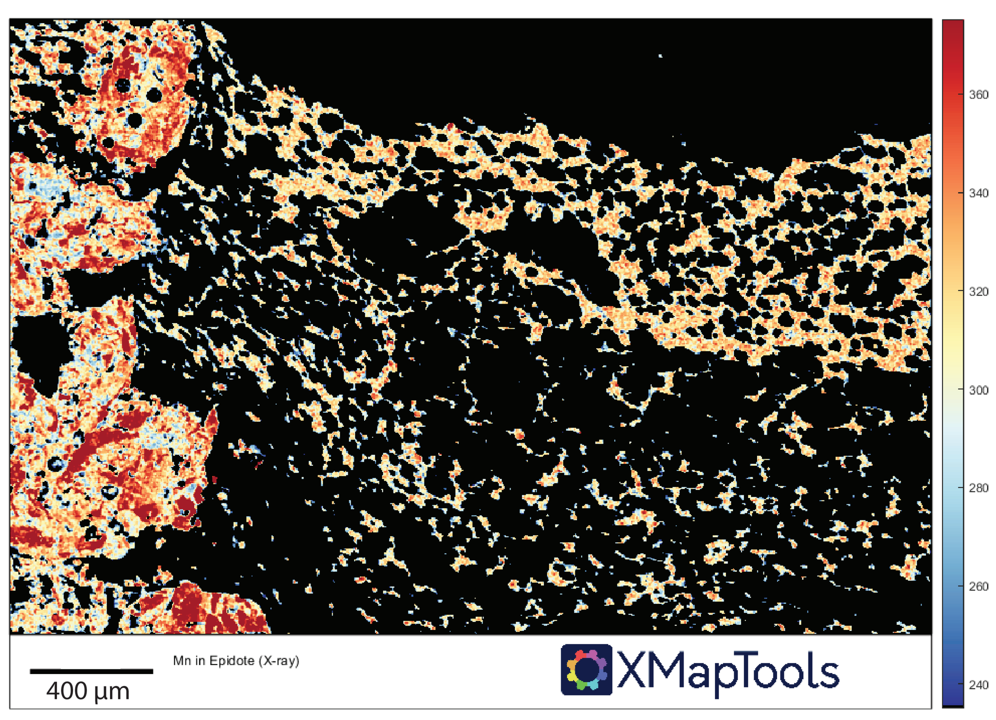

Fig. 8- Qualitative chemical map of Mn in the analyzed epidote vein.

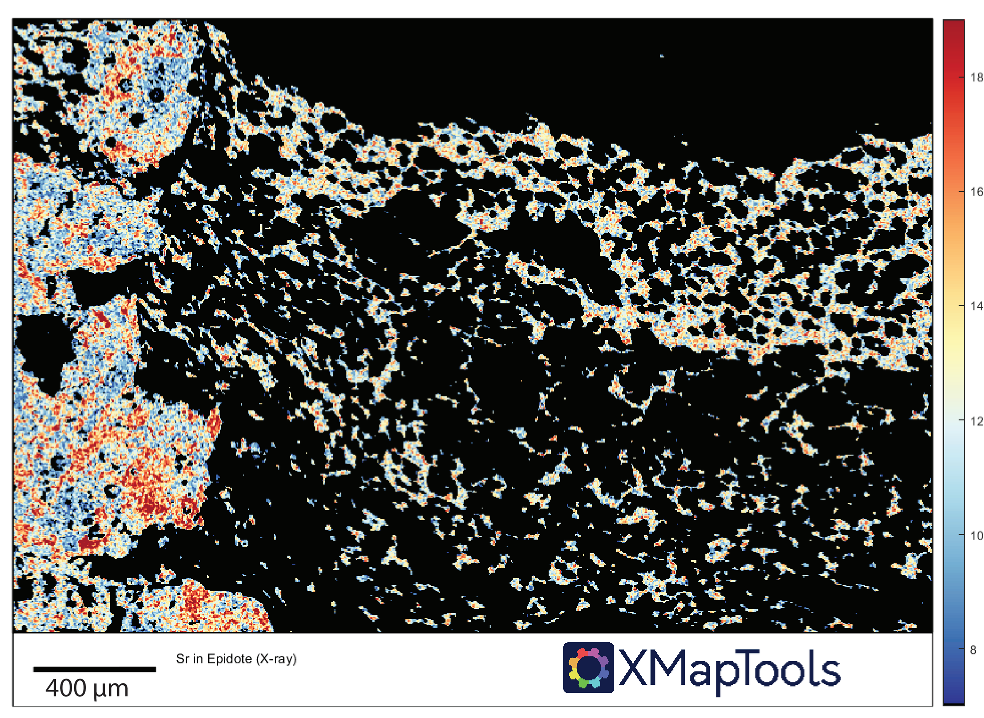

Fig. 9- Qualitative chemical map of Sr in the analyzed epidote vein.

5 Possible scenarios for the formation of Epidote-B

1) Crystallization from an external fluid.
2) Resulting from grain-size reduction of Epidote-A.
3) Resulting from dissolution of Epidote-A and precipitation.

The absence of a phyllosilicate associated with Epidote-B (Fig. 1) supports Epidote-A and -B representing two successive events of epidote crystallization. However, Epidote-B defines a fold whose limbs are connected to Epidote-A (Fig. 1), therefore arguing for the genesis of Epidote-B being somehow linked to Epidote-A.

The genetic link of Epidote-B with Epidote-A is further supported by the consistency in REE patterns between the two epidote generations (Fig. 6). The loss of chemical variability in Epidote-B in comparison with Epidote-A (Figs. 7-9), seems inconsistent with Epidote-B resulting from grain-size reduction of Epidote-A. Instead, **the geochemical and microstructural data support that Epidote-B resulted from dissolution of Epidote-A by an external fluid with different isotopic characteristics than Epidote-A (Fig.5), which mediated the folding of the vein and the precipitation of Epidote-B.**

References:
[1] Peverelli et al., Geochronology 3, 123-147, 2021.
[2] Dahl, EPSL 150, 277-290, 1997.
[3] Wehrens et al., J.Struct.Geol. 94, 47-67, 2017.